ELSEVIER

Carbohydrate Research 337 (2002) 935–945

CARBOHYDRATE RESEARCH

www.elsevier.com/locate/carres

Hexasaccharides from the histamine-modified depolymerization of porcine intestinal mucosal heparin

Wei-Lien Chuang, Heather McAllister, Dallas L. Rabenstein*

Department of Chemistry, University of California, Riverside, CA 92521, USA

Received 16 August 2001; accepted 12 February 2002

Abstract

Specific sequences in heparin are responsible for its modulation of the biological activity of proteins. As part of a program to characterize heparin–peptide and heparin–protein binding, we are studying the interaction of chemically discrete heparin-derived oligosaccharides with peptides and proteins. We report here the isolation and characterization, by one- and two-dimensional ^{1}H NMR spectroscopies, of ten hexasaccharides, one pentasaccharide, and one octasaccharide serine that were isolated from depolymerized porcine intestinal mucosal heparin. Hexasaccharides were chosen for study because they fall within the size range, typically tetra- to decasaccharide in length, of heparin sequences that modulate the activity of proteins. The depolymerization reaction was catalyzed by heparinase I (EC 4.2.2.7) in the presence of histamine, which binds site specifically to heparin. Histamine increases both the rate and extent of heparinase I-catalyzed depolymerization of heparin. It is proposed that oligosaccharides produced by heparinase I-catalyzed depolymerization can inhibit the enzyme by binding to the imidazolium group of histidine-203, which together with cysteine-135 forms the catalytic domain of heparinase I. The increased rate and extent of depolymerization are attributed to competitive binding of the oligosaccharides by histamine.

Keywords: Heparin; Hexasaccharides; Heparinase I; Histamine

1. Introduction

Heparin is a highly sulfated, linear polysaccharide with a wide range of biological activities, including inhibition of blood coagulation,[1] release of lipoprotein lipase and hepatic lipase,[2,3] inhibition of complement activation,[4,5] regulation of cell proliferation,[6,7] inhibition of angiogenesis and tumor growth,[8,9] and antiviral activity.[10,11] These activities result from the interaction of heparin with proteins,[12] the most well characterized being its interaction with antithrombin.[1,13,14] With the discovery that the anticoagulant activity of heparin resides in a unique pentasaccharide sequence with antithrombin binding properties,[15–19] there has been intense interest in characterizing the primary structure of heparin and the contribution of unique oligosaccharide sequences to its various biological activities.[20–25] However, identification of oligosaccharide sequences in heparin with specific biological activities has been difficult due to its structural heterogeneity.

The basic polymeric structure of heparin consists of alternating (1→4)-linked glucosamine and uronic acid residues. The major repeating unit is the trisulfated disaccharide GlcNS(6S)–IdoA(2S), where GlcNS(6S) represents *N*- and 6-*O*-sulfated glucosamine and IdoA(2S) represents 2-*O*-sulfated iduronic acid. This repeating disaccharide accounts for at least 85% of heparins from bovine lung and 75% of those from porcine intestinal mucosa.[26,27] Structural microheterogeneity is present in the other parts of heparin due to incomplete pathways in its biosynthesis, including incomplete epimerization of glucuronic acid to iduronic acid, *O*-sulfation and *N*-deacetylation/*N*-sulfation. The structural diversity of heparin gives rise to its wide range of biological activities.

In this paper, we report structures and ^{1}H NMR spectral data for ten hexasaccharides, one pentasaccha-

* Corresponding author. Tel.: +1-909-7873585; fax: +1-909-7872435.

E-mail address: dlrab@mail.ucr.edu (D.L. Rabenstein).

0008-6215/02/$ - see front matter
PII: S0008-6215(02)00050-2

ride and one octasaccharide serine from the carbohydrate–protein linkage region. The oligosaccharides were obtained by heparinase I-catalyzed depolymerization of porcine intestinal mucosal heparin.[28,29] Enzymatic depolymerization with heparinases offers the advantage that the cleavage conditions are sufficiently mild that the fine structure of the oligosaccharides is not altered.[30] However, some oligosaccharide sequences are either absent or present in very small quantities because of the substrate specificity of the heparin lyases.[13] To enrich the production of some oligosaccharide sequences, histamine, which binds site-specifically to heparin,[31,32] was added to the depolymerization solutions.[33] This resulted in the isolation and characterization of four hexasaccharides not previously reported.

The purpose of this work was to isolate and characterize chemically discrete heparin-derived oligosaccharides for use in our studies of the interaction of peptides and proteins with heparin, while at the same time providing new information about the primary structure of heparin. We have chosen hexasaccharides for the first phase of this study because they fall within the size range of heparin sequences, typically from tetra- to decasaccharide in length, that are responsible for modulation of the biological activity of proteins.[34]

2. Experimental

Materials.—Histamine hydrochloride, *Flavobacterium* heparinase I (EC 4.2.2.7) and the sodium salt of porcine intestinal mucosal heparin were obtained from Sigma Chemical Co. Bio-Gel P6 gel-permeation chromatography (GPC) matrix was purchased from BioRad Laboratories, Richmond, CA. Sephadex G10 and G15 were obtained from Pharmacia Biotech, Piscataway, NJ. The Superdex Peptide HR GPC column (10 × 300 mm) was obtained from Pharmacia Biotech, Piscataway, NJ. Strong anion exchange (SAX)-HPLC was performed on CarboPac PA1 columns (4 × 250 mm and 9 × 250 mm) from Dionex, Sunnyvale, CA. HPLC separations were performed on a Dionex 500 ion-chromatography system equipped with a GP40 gradient pump and an AD20 UV–Vis detector. Water was purified with a Millipore water purification system. All other reagents and chemicals were of the highest quality available. NMR experiments were performed at 500 MHz and 10–25 °C on a Varian Unity Inova spectrometer equipped with a $^{1}H\{^{13}C,^{15}N\}$ triple resonance, *X,Y,Z* triple axis pulsed field gradient probe. Shigemi NMR tubes were obtained from Shigemi Co., Inc. Sodium 3-(trimethylsilyl)propionate-2,2,3,3-D_4 (TSP) was obtained from Aldrich Chemical Co.

Enzymatic depolymerization of heparin.—Porcine intestinal mucosal heparin was cleaved by digestion with heparinase I.[28,29,35,36] Depolymerization solutions contained 0.1 M sodium acetate, 30 mM calcium acetate, and 0.02% sodium azide. To determine optimum conditions for depolymerization in the presence of histamine, the reaction was run on a small scale and monitored by two-dimensional chromatography.[33] A 100-mg sample of heparin was digested with 25 U of heparinase I (Sigma units, 1 U is defined as the quantity of enzyme that will form 0.1 μmol of unsaturated uronic acid product per h at pH 7.5 and 25 °C) in 2 mL of pH 7.5 depolymerization solution without histamine and at histamine–heparin ratios of 2:1, 4:1, and 10:1, where the mole ratio is defined in terms of the concentration of the heparin repeating disaccharide. Aliquots (100 μL) of the reaction mixtures were size-separated on a Superdex GPC column with a 0.2 M NaCl eluent at a flow rate of 0.7 mL/min. The absorbance was measured at 232 nm (Fig. 1). The peak corresponding to the hexasaccharide fraction was collected for further analysis by SAX-HPLC. A 100-μL aliquot was injected directly onto the analytical-scale CarboPac PA1 column. Oligosaccharides were eluted with a linear gradient of 70 mM pH 3 (or 7) phosphate buffer (solvent A) and 70 mM pH 3 (or 7) phosphate buffer containing 2 M NaCl (solvent B) at a flow rate of 1.2 mL/min.

Based on the results in Fig. 1, preparative-scale reactions were run using a histamine–heparin ratio of 4:1. Heparin (1 g), histamine hydrochloride (928 mg), and 250 units of heparinase I were dissolved in 50 mL of depolymerization solution. When the absorbance at 232 nm reached a plateau (typically after 200 h for these conditions), the reaction was stopped and the solution was concentrated by lyophilization. The lyophilized product was size-fractionated by gravity flow GPC on a 3 × 200-cm Bio-Gel P6 column using a 0.5 M NH_4HCO_3 eluent at a flow rate of 8–12 mL/h. Fractions (2.0 mL) were collected and the absorbance of each fraction was measured at 232 nm. From peak areas in the resulting chromatogram, the hexasaccharide fraction was ~10% of the total depolymerization product. The hexasaccharide fractions from multiple runs were pooled.

The hexasaccharide solution was desalted by lyophilization and then separated by SAX-HPLC with a semipreparative scale CarboPac PA1 column. A representative chromatogram is shown in Fig. 2. To increase efficiency of the isolation of pure hexasaccharides, a two-step procedure was used that allowed the injection of larger amounts. In the first step, 10 mg of the hexasaccharide fraction was injected onto the semipreparative scale CarboPac column; a representative chromatogram is shown in Fig. 3(A). The resolution is less than that in Fig. 2 because the column was overloaded. Fractions were collected (fraction 1 from 8–32 min and fractions **A**–**G**, **J** and **K** as indicated). Fraction 1 from multiple separations was

pooled and then rechromatographed using a different gradient; a representative chromatogram is shown in Fig. 3(B). Peaks labeled **H**, **I**, and **L** were collected. Fractions **A**–**L** were purified further by combining several well-separated fractions, diluting to reduce the NaCl concentration to below 0.4 M, and then pumping the entire solution through the CarboPac column as the mobile phase. The oligosaccharides stayed on the column while the NaCl was eluted. The oligosaccharides were then eluted with a NaCl gradient. To illustrate, chromatogram C in Fig. 3 was obtained for a mixture of **B**, **D**, **F**, **G**, **J**, and **K** by this procedure. The NaCl was then removed from each purified oligosaccharide solution by GPC on a 10×500 mm Sephadex G-10 column using Millipore water as the eluent. Fractions (1.5 mL) were collected and monitored by both conductivity and absorbance at 232 nm. The desalted oligosaccharides were lyophilized, and their purity was checked by ^{1}H NMR spectroscopy. If there was greater than 20% impurity, the oligosaccharide was repurified.

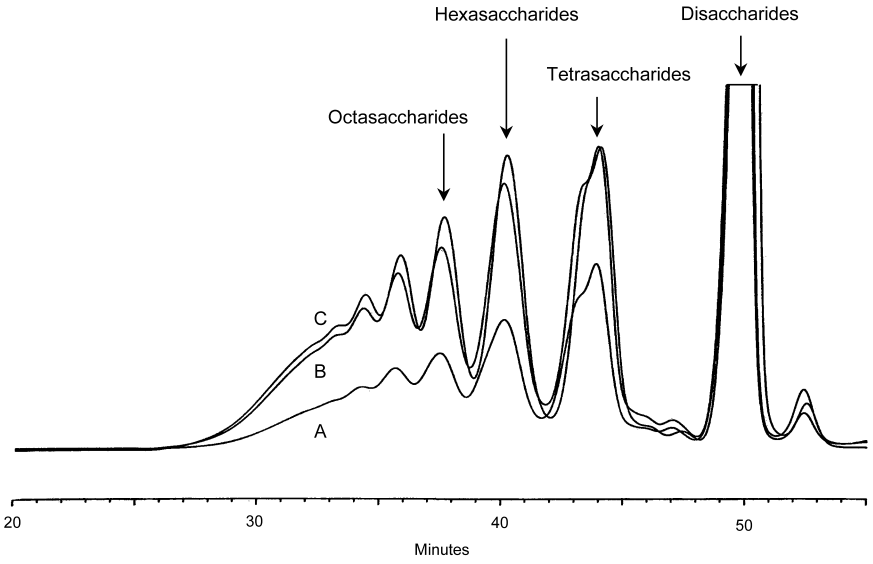

Fig. 1. Size fractionation of depolymerized porcine intestinal mucosal heparin by high-performance GPC on a Superdex column (eluent: 0.2 M NaCl; flow rate: 0.7 mL/min). The heparin was depolymerized (A) without histamine; (B) at a histamine–heparin disaccharide ratio of 2:1; and (C) at a histamine–heparin disaccharide ratio of 4:1. The chromatograms are for 100 μL aliquots after 200 h of reaction. At a histamine–heparin disaccharide ratio of 10:1, there was very little depolymerization product (data not shown).

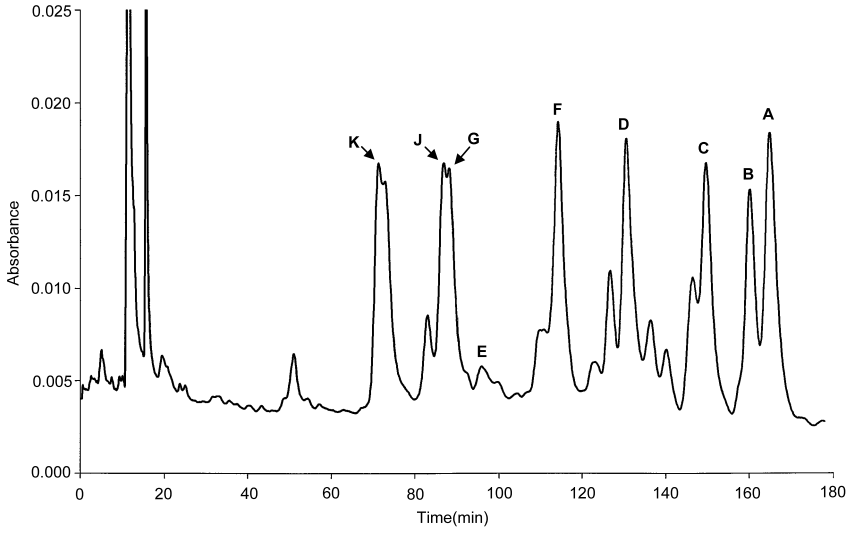

Fig. 2. A SAX-HPLC chromatogram of $\sim$1.0 mg of the hexasaccharide fraction. The letters identify nine of the 12 fractions isolated by the procedure outlined in Fig. 2. A linear gradient was formed from 70 mM NaH_2PO_4 at pH 3.0 (solvent A) and 2.0 M NaCl + 70 mM NaH_2PO_4 at pH 3.0 (solvent B). The gradient started at 100% solvent A, with the amount of solvent B increased at a rate of 4.5%/min for 10 min, and then 0.33%/min.

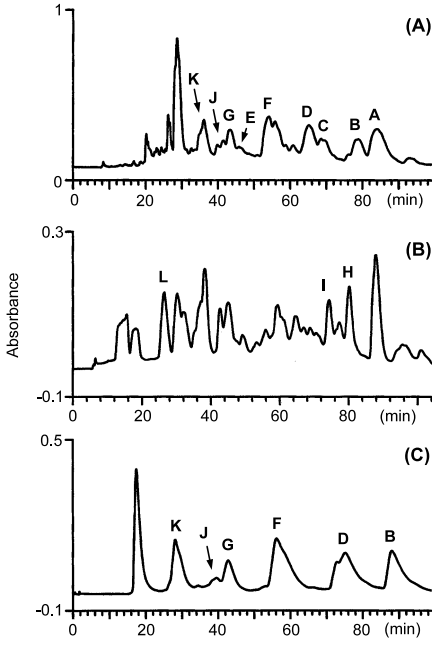

Fig. 3. Isolation of oligosaccharides by SAX-HPLC on a semipreparative scale CarboPac PA1 column. The letters identify the fractions collected; the oligosaccharides in these fractions are identified in Table 2. A two-step procedure was used in which fractions were collected, combined and then rechromatographed to increase the purity of the isolated oligosaccharides (see text for details). Linear gradients were formed from 70 mM NaH_2PO_4 at pH 3.0 (solvent A) and 2.0 M sodium chloride + 70 mM NaH_2PO_4 at pH 3.0 (solvent B). (A) Chromatogram for ~10 mg of the hexasaccharide fraction. The gradient started at 100% solvent A, with the amount of solvent B increased at a rate of 4.5%/min for 10 min, and then 0.33%/min. (B) Chromatogram for fraction 1. The gradient started at 100% solvent A, with the amount of solvent B increased at a rate of 2.5%/min for 10 min, and then 0.33%/min. (C) The chromatogram for repurification of fractions **B**, **D**, **F**, **G**, **J**, and **K**. The gradient started at 20% solvent B, which was increased at a rate of 3%/min for 10 min, and then 0.33%/min.

The quantities obtained from the depolymerization of 1 g of porcine heparin were: ~15 mg for **A**, 7 mg for **B**, 3 mg for **C** and **F**, 4 mg for **D**, 5 mg for **K**, 1 mg for **E**, **H**, **I**, **J** and **L**, and 2 mg for **G**.

NMR procedures.—The pure oligosaccharides were lyophilized in D_2O three times to replace exchangeable protons with deuterium. They were then dissolved in 320 μL of D_2O containing TSP for a chemical shift reference. The sample solution was filtered through a 0.45-μm Microspin filter and transferred to a Shigemi NMR tube. A one-dimensional ^1H NMR spectrum and two-dimensional correlation spectroscopy (COSY), double quantum filtered correlation spectroscopy (DQF-COSY), total correlation spectroscopy (TOCSY) and rotating frame Overhauser effect spectroscopy (ROESY) ^1H NMR spectra were measured for each sample.[37–40] Spectra were measured at 25 °C, unless otherwise specified. A 10-ppm spectral width was used for measuring 1D spectra, and a 6-ppm spectral width for 2D spectra. Selective presaturation was used to reduce the intensity of the HDO resonance. Two-dimensional data sets were acquired with 4096 points in the t_2 dimension and 256–512 increments in the t_1 dimension; a 60–90° shifted sine-bell squared apodization was applied to both dimensions to drive the FID to zero at the last point. A baseline correction was applied after the first (t_2) Fourier transform.

3. Results

Heparinase I catalyzes cleavage of the glucosaminidic linkage in the GlcNS(±6S)–uronic acid–GlcNS(±6S) sequence of heparin.[25,42] Histamine modifies the heparinase I-catalyzed depolymerization, with a decrease in the production of some oligosaccharides and an increase in the production of others.[33] To determine if histamine alters the rate of the heparinase I-catalyzed reaction, the reaction was monitored by ^1H NMR spectroscopy. The anomeric region of representative spectra measured as a function of time at a histamine–heparin ratio of 4:1 (A) and with no histamine present (B) are presented in Fig. 4. The patterns of resonances for the anomeric (H-1) protons (5.0–5.7 ppm) and for the H-4 proton of the unsaturated uronic acid residue (ΔUA) formed by the cleavage reaction (5.95–6.01 ppm) are different in the presence of histamine, which provides evidence that the cleavage pattern is modified by histamine, including a significant increase in the amount of ΔUA(2S)-(1→4)-GlcNS(6S) disaccharide formed, as indicated by the increased intensity of the

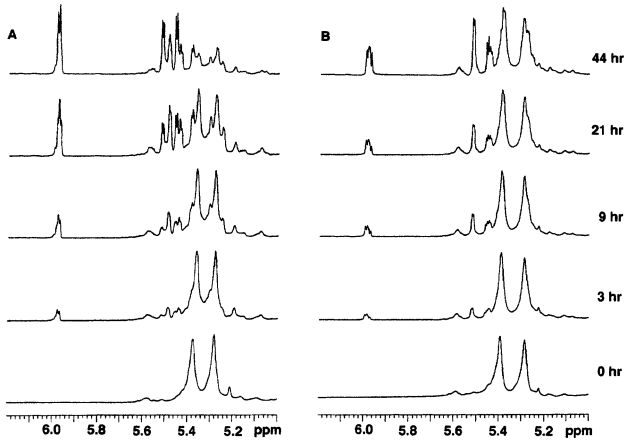

Fig. 4. Portions of ^1H NMR spectra measured as a function of time for depolymerization solutions which contained (A) histamine at a histamine–heparin disaccharide repeat unit ratio of 4:1 and (B) no histamine. Heparin (50 mg) and 50 units of heparinase I were dissolved in 2 mL of D_2O solution containing 100 mM sodium acetate and 10 mM calcium acetate at pD 7.1. The depolymerization reactions were run at 30 °C.

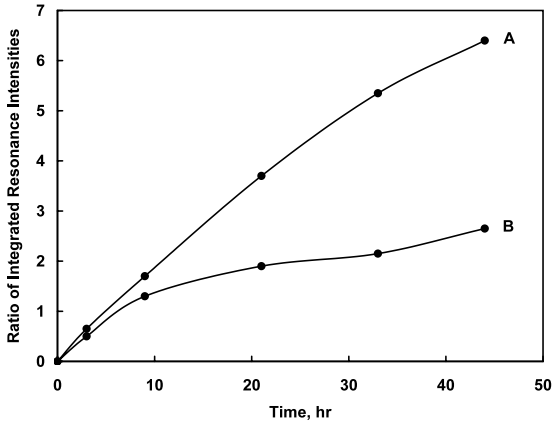

Fig. 5. The ratio of the integrated intensities of the resonances for the H-4 protons of the ΔUA residues (5.95–6.01 ppm in Fig. 3) of the oligosaccharides formed by heparinase I-catalyzed depolymerization of heparin and the methyl resonance of the internal TSP. The depolymerization reaction conditions are given in the legend to Fig. 3. (A) Histamine present at a histamine–heparin disaccharide repeat unit ratio of 4:1 and (B) no histamine.

resonances for its H-1 protons at 5.52 and 5.46 ppm. The progress of the depolymerization reaction was characterized by taking the ratio of the integrals for the H-4 resonance of the ΔUA residue and the methyl resonance of the internal TSP. The results in Fig. 5 indicate that the rate of reaction is increased in the presence of histamine, while the results in Fig. 1 indicate that the extent of reaction is also increased by histamine.

Structural characterization of heparin-derived oligosaccharides.—Twelve oligosaccharides (**A**–**L**) were isolated in sufficient quantity and purity for structure characterization by ^{1}H NMR spectroscopy. Their structures were determined using a combination of data obtained from one- and two-dimensional ^{1}H NMR spectra. The procedure will be illustrated with the assignment of the structure of oligosaccharide **K**. The one-dimensional ^{1}H NMR spectrum of **K** is shown in

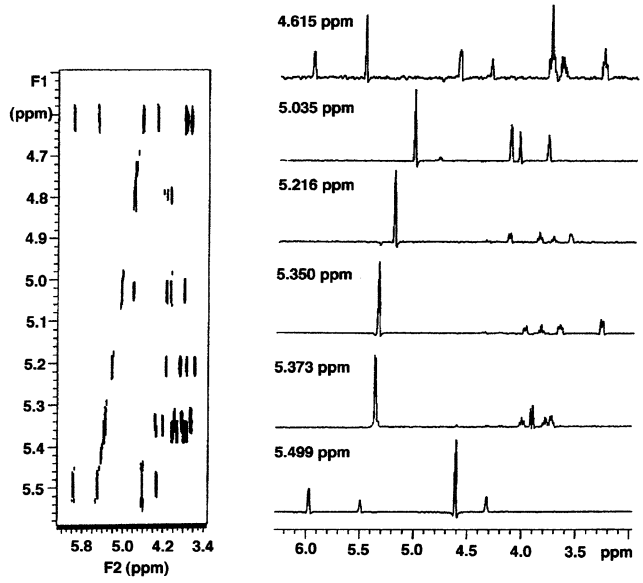

Fig. 7. A portion of the TOCSY spectrum of oligosaccharide **K** and subspectra obtained by taking traces through the TOCSY spectrum at the chemical shifts of the anomeric proton resonances. 4 K data points were collected at 256 t_1 increments using a mixing time of 120 ms.

Fig. 6. The resonance at 5.978 ppm is for the H-4 proton of the ΔUA residue. The five resonances in the 5.0–5.6 ppm region are for anomeric (H-1) protons. The identity of the monosaccharide residue giving each anomeric resonance was determined using subspectra obtained by taking traces through two-dimensional TOCSY spectra at the chemical shifts of the H-1 resonances (Fig. 7). The resonance at 5.978 ppm in the subspectrum taken at 5.499 ppm indicates the H-1 resonance at 5.499 ppm is for the ΔUA residue. The other subspectra indicate the H-1 resonances at 5.373 and 5.350 ppm are for glucosamine residues, while those at 5.216 and 5.035 ppm are for uronic acid residues.[41] The 1D spectrum shows that there are two partially overlapped resonances at 4.614 and 4.615

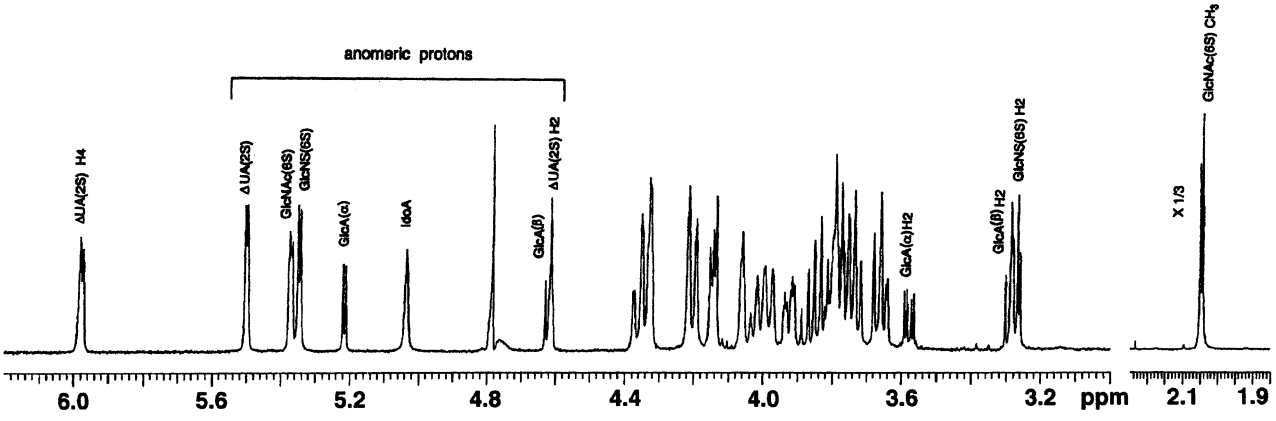

Fig. 6. 500 MHz ^{1}H NMR spectrum of oligosaccharide **K** in D_2O solution.

Table 1
^{1}H chemical shift data for the constituent monosaccharides of the heparin-derived oligosaccharides [a]

Monosaccharide [b]	Proton	A	B	C	D	E	F	G	H	I	J	K	L [c]
ΔUA-a	H-1	5.512	5.502	5.511	5.506	5.515	5.519	5.512	5.532	5.515	5.499	5.499	5.500
	H-2	4.637	4.616	4.629	4.624	4.629	4.634	4.628	4.605	4.630	4.624	4.614	4.620
	H-3	4.315	4.320	4.320	4.309	4.303	4.318	4.320	4.226	4.319	4.316	4.326	4.323
	H-4	5.988	6.007	5.990	5.983	5.985	5.991	5.992	6.028	5.987	5.980	5.978	5.980
GlcN-b	H-1	5.421	5.369	5.420	5.438	5.317	5.343	5.410	5.324	5.333	5.357	5.350	5.394
	H-2	3.290	3.297	3.300	3.289	3.290	3.298	3.303	3.279	3.296	3.268	3.274	3.287
	H-3	3.648	3.654	3.660	3.629	3.672	3.668	3.657	3.672	3.666	3.632	3.660	3.622
	H-4	3.853	3.832	3.840	3.828	3.837	3.838	3.841	3.785	3.837	3.834	3.832	3.824
	H-5	4.048	4.010	4.060	4.043	4.023	4.029	4.048	3.823	4.928	3.981	3.973	3.989
	H-6a	4.362	4.361	4.260	4.350	4.240	4.350	4.275	3.840	4.349	4.220	4.362	4.352
	H-6b	4.263	4.239	4.370	4.260	4.348	4.250	4.344	ND [d]	4.244	4.310	4.218	4.216
HexA-c	H-1	5.203	5.233	5.220	5.204	5.238	5.230	5.219	5.241	5.225	4.990	5.035	4.941
	H-2	4.335	4.336	4.350	4.325	4.330	4.341	4.337	4.325	4.330	3.768	3.792	3.718
	H-3	4.215	4.245	4.220	4.207	4.250	4.251	4.222	4.264	4.250	4.125	4.145	4.111
	H-4	4.099	4.084	4.110	4.098	4.040	4.059	4.098	4.038	4.050	4.060	4.053	4.076
	H-5	4.817	4.868	4.830	4.768	4.860	4.815	4.814	4.954	4.840	4.770	4.860	4.735
GlcN-d	H-1	5.465	5.577	5.402	5.391	5.388	5.367	5.383	5.394	5.365	5.388	5.373	5.355
	H-2	5.280	3.272	3.290	3.925	3.246	3.913	3.269	3.237	3.240	3.928	3.915	3.901
	H-3	3.648	3.660	3.670	3.771	3.660	3.786	3.653	3.650	3.650	3.773	3.780	3.750
	H-4	3.760	3.751	3.780	3.766	3.700	3.713	3.766	3.696	3.830	3.721	3.739	3.820
	H-5	4.032	3.968	4.020	3.976	3.880	3.840	3.985	3.830	3.920 [e]	4.015	4.017	3.710
	H-6a	4.380	4.351	4.270	4.410	3.910	ND	4.250	3.860	3.790 [e]	4.330	4.198	ND
	H-6b	4.270	4.288	4.410	4.250	3.910	ND	4.381	ND	ND	4.200	4.350	ND
	NAc	NA [d]	NA	NA	2.046	NA	2.051	NA	NA	NA	2.047	2.047, 2.054 [f]	2.041
HexA-e	H-1	5.199	4.616	5.200	4.589	5.200	4.591	4.969	5.197	4.973	4.581	5.216, 4.615 [f]	4.647
	H-2	4.314	3.391	4.320	3.342	4.300	3.341	3.722	4.302	3.710	3.380	3.587, 3.282	3.419
	H-3	4.176	3.840	4.210	3.718	4.210	3.738	4.118	4.214	4.130	3.725	3.871, 3.652	3.708
	H-4	4.133	3.794	4.110	3.763	4.090	3.752	4.098	4.079	4.072	3.752	3.720, 3.753	3.756
	H-5	4.741	3.810	4.780	3.822	4.770	3.829	4.740	4.841	4.730	3.819	4.143, 3.769	ND
GlcN-f	H-1	5.457	5.447	5.460	5.472	5.458	5.477	5.212, 4.713 [f]	5.456	5.216, 4.702 [f]	5.474	NA	
	H-2	3.267	3.270	3.250	3.272	3.243	3.285	3.900, 3.692	3.238	3.888, 3.687	3.277	NA	
	H-3	3.700	3.724	3.680	3.732	3.690	3.753	3.830, 3.574	3.870	3.825, 3.571	3.718	NA	
	H-4	3.750	3.735	3.720	3.698	3.720	3.702	3.730, 3.630	3.717	3.710, 3.804	3.735	NA	
	H-5	4.137	4.143	3.689	4.153	3.930	4.165	3.960, 3.810	3.689	3.962, 3.912	4.166	NA	
	H-6a	4.380	4.360	3.927	4.350	3.910	4.350	ND, 3.910	3.950	ND, ND	4.320	NA	
	H-6b	4.319	4.300	3.930	4.350	3.910	4.350	ND, ND	3.950	ND, ND	4.320	NA	
	NAc	NA	NA	NA	NA	NA	NA	2.049, 2.049	NA	2.045, 2.045	NA	NA	

[a] Chemical shifts are reported in ppm relative to internal TSP. Estimated uncertainties are ± 0.002 ppm.

[b] The lower case letter in ΔUA-a, GlcN-b, etc denotes the position of the residue in the oligosaccharide, starting with the residue at the nonreducing end.

[c] Oligosaccharide **L** also contains the linker sequence Gal1–Gal2–Xyl3–Ser. For Gal1, H-1 (4.670 ppm), H-2 (3.680), H-3 (3.752), H-4 (4.170); for Gal2, H-1 (4.543), H-2 (3.680), H-3 (3.830), H-4 (4.200); for Xyl, H-1 (4.456), H-2 (3.403), H-3 (3.622), H-4 (3.880), H-5a (4.11), H-5b (3.39); for Ser, $C_\alpha H$ (4.258), $C_\beta Ha$ (4.066), $C_\beta Hb$ (4.096).

[d] ND, not determined; NA, not applicable.

[e] Assignments not determined.

[f] The first number is for the α conformer, the second is for the β conformer.

ppm. Cross peaks in subspectra taken at 5.499 and 4.614 ppm on the *F*2 axis indicate that the resonance at 4.614 ppm is for a proton of the ΔUA residue. However, the resonance at 4.615 ppm is for the anomeric proton of a uronic acid residue of a low-abundance isomer as indicated by the pattern of resonances in TOCSY subspectra.

Resonances in the TOCSY subspectra were assigned to specific protons in each monosaccharide using cross peaks in the DQF-COSY spectrum (data not shown). The sequence of the monosaccharides was then determined using H-1/H-4 and H-4/H-1 cross peaks in the ROESY spectrum (Fig. 8), starting with the cross peak to H-1 of the ΔUA residue.[41] Taken together, these data indicate the core oligosaccharide to be ΔUA–GlcN–IdoA–GlcN–GlcA, where GlcN, IdoA and GlcA represent α-D-glucosamine, α-L-iduronic acid and D-glucuronic acid, respectively. The chemical shift data are summarized in Table 1.

The GlcA at the reducing end can exist in both the α and β anomers; the chemical shifts of the H-1 resonances for the two anomers are ~5.2 and 4.62 ppm, respectively.[42,43] Thus, the H-1 resonances at 5.215 and 4.615 ppm are assigned to the α and β anomers of the GlcA residue at the reducing end of **K**.

The substituents on the monosaccharides were identified by comparison of the chemical shift data in Table 1 to reference chemical shift data in the literature.[23–25,41–48] Starting at the nonreducing end, the chemical shift of the resonance for H-2 of ΔUA indicates a 2-*O*-sulfate group. The chemical shift of 3.274 ppm for H-2 of the GlcN residue linked to ΔUA(2S) (GlcN-b, where b represents position in the oligosaccharide sequence, starting with residue ΔUA-a at the nonreducing terminus) indicates an *N*-sulfate group, while the chemical shifts of 4.218 and 4.362 ppm for the resonances for the H-6 proton indicate a 6-*O*-sulfate group. The chemical shifts of the H-1 and H-3 protons of the ΔUA(2S) residue provide additional evidence for a 6-*O*-sulfate group.[45] The chemical shift of 3.796 ppm for H-2 of IdoA-c indicates an OH group at the 2-position. The chemical shift of 3.924 ppm for H-2 of GlcN-d indicates an *N*-acetyl group, while the chemical shifts of 4.204 and 4.336 ppm for the H-6 protons indicate a 6-*O*-sulfate group. The presence of an *N*-acetyl group is also indicated by two resonances at 2.047 and 2.054 ppm, with a total integrated intensity consistent with one acetyl group. Finally, the chemical shift of 3.282 ppm for H-2 of the β conformer of the GlcA residue indicates an OH group at the 2-position. Taken together, these results indicate that **K** is (1→4)-linked ΔUA(2S)–GlcNS(6S)–IdoA–GlcNAc(6S)–GlcA(α,β) (Table 2). The ratio of the α to β anomers was determined to be ~3 to 2 from the integrated intensities of the resonances at 5.216 and 4.615 ppm and the integrated intensities of the two acetyl resonances at 2.047 and 2.054 ppm. The same structure has been reported

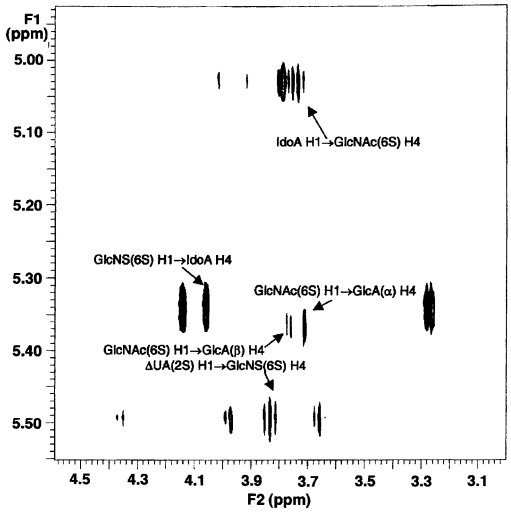

Fig. 8. A portion of the ROESY spectrum of oligosaccharide **K**. The dipolar cross peaks which establish the sequence of the monosaccharide residues are identified. 4 K data points were collected at 256 t_1 increments using a mixing time of 120 ms.

Table 2
Structures of the oligosaccharides isolated from the histamine-modified depolymerization of porcine intestinal mucosal heparin [a]

Fraction	Structure
A	ΔUA(2S)–GlcNS(6S)–IdoA(2S)–GlcNS(6S)–IdoA(2S)–GlcNS(6S)
B	ΔUA(2S)–GlcNS(6S)–IdoA(2S)–GlcNS(6S)–GlcA–GlcNS(6S)
C	ΔUA(2S)–GlcNS(6S)–IdoA(2S)–GlcNS(6S)–IdoA(2S)–GlcNS
D	ΔUA(2S)–GlcNS(6S)–IdoA(2S)–GlcNAc(6S)–GlcA–GlcNS(6S)
E	ΔUA(2S)–GlcNS(6S)–IdoA(2S)–GlcNS–IdoA(2S)–GlcNS
F	ΔUA(2S)–GlcNS(6S)–IdoA(2S)–GlcNAc–GlcA–GlcNS(6S)
G	ΔUA(2S)–GlcNS(6S)–IdoA(2S)–GlcNS(6S)–IdoA–GlcNAc
H	ΔUA(2S)–GlcNS–IdoA(2S)–GlcNS–IdoA(2S)–GlcNS
I	ΔUA(2S)–GlcNS(6S)–IdoA(2S)–GlcNS–IdoA–GlcNAc
J	ΔUA(2S)–GlcNS(6S)–IdoA–GlcNAc(6S)–GlcA–GlcNS(6S)
K	ΔUA(2S)–GlcNS(6S)–IdoA–GlcNAc(6S)–GlcA(α,β)
L	ΔUA(2S)–GlcNS(6S)–IdoA–GlcNAc–GlcA–Gal–Gal–Xyl–Ser

[a] 2S, 6S, and NS represent 2-*O*-, 6-*O*-, and 2-*N*-sulfate, and NAc represents 2-*N*-acetyl.

by Yamada et al. based on more limited NMR data.[42] A comparison of the chemical shift data in Table 1 for oligosaccharide **K** with that reported by Yamada et al. shows agreement within 0.04 ppm.

^{1}H chemical shift data for the other oligosaccharides are also reported in Table 1 and their structures are given in Table 2. The twelve oligosaccharides include ten hexasaccharides, one pentasaccharide, and one octasaccharide serine from the protein linkage region. Hexasaccharides **E**, **G**, **H**, and **I** have not been reported previously.

Hexasaccharide **A**.—Hexasaccharide **A** consists of three fully sulfated disaccharide repeat units: ΔUA(2S)–GlcNS(6S)–IdoA(2S)–GlcNS(6S)–IdoA(2S)–GlcNS(6S). The chemical shift data in Table 1 are in good agreement with that reported in previous studies.[23,24,35,36]

Hexasaccharide **B**.—The presence of a D-glucuronic acid residue in **B** is indicated by the characteristic chemical shift of H-1 (4.616 ppm), a characteristic triplet for H-2 at 3.391 ppm, and a $^3J_{1,2}$ coupling constant of ~8.5 Hz. The ^{1}H NMR spectrum of **B** indicates the ratio of the monosaccharides ΔUA(2S), IdoA(2S), GlcA, and GlcNS(6S) to be 1:1:1:3. The saccharide sequence was determined from the ROESY spectrum to be ΔUA(2S)–GlcNS(6S)–IdoA(2S)–GlcNS(6S)–GlcA–GlcNS(6S). The chemical shifts in Table 1 for **B** are in agreement with reported values.[23,24,35]

Hexasaccharide **C**.—There are anomeric H-1 resonances for one ΔUA(2S) residue (5.511 ppm), two IdoA(2S) residues (5.220 and 5.200 ppm) and three glucosamine residues (5.420, 5.402, and 5.460 ppm) in the 1D spectrum of **C**. The TOCSY spectrum is similar to that of **A** except that the resonances for the two H-6 protons of one glucosamine residue are 0.4 ppm upfield from those for GlcNS(6S), which indicates the absence of a 6-*O*-sulfate group.[41] Using these results together with data from the ROESY spectrum, the structure was determined to be: ΔUA(2S)–GlcNS(6S)–IdoA(2S)–GlcNS(6S)–IdoA(2S)–GlcNS.

Hexasaccharides **E** *and* **H**.—Chemical shift data for **E** and **H** indicate they have structures similar to **C**, with the exception that the TOCSY subspectra indicate **E** has two glucosamine residues that lack 6-*O*-sulfate groups, while all three glucosamine residues of **H** lack 6-*O*-sulfate groups. Using connectivities in the ROESY spectrum, the structure of **E** was determined to be ΔUA(2S)–GlcNS(6S)–IdoA(2S)–GlcNS–IdoA(2S)–GlcNS; that of **H** was determined to be ΔUA(2S)–GlcNS–IdoA(2S)–GlcNS–IdoA(2S)–GlcNS. **E** and **H** have not been reported previously.

Hexasaccharide **D**.—The methyl resonance at 2.03 ppm and the downfield shift for an H-2 resonance indicates a GlcNAc residue in **D**. There is one glucuronic acid residue, as indicated by an H-1 resonance at 4.589 ppm ($^3J_{1,2}$ 8.0 Hz) and an H-2 resonance at 3.342 ppm ($^3J_{2,3}$ 9.4 Hz). The chemical shift data indicate that the other four residues are fully sulfated iduronic acid and glucosamine. The integrated intensities of the H-1 resonances indicate that ΔUA(2S), IdoA(2S), GlcA, GlcNS(6S), and GlcNAc(6S) are present in a 1:1:1:2:1 ratio. Using sequence information from the ROESY spectrum, the structure was determined to be ΔUA(2S)–GlcNS(6S)–IdoA(2S)–GlcNAc(6S)–GlcA–GlcNS(6S). The chemical shift data are in agreement with data reported previously for **D**.[44]

Hexasaccharides **F** *and* **J**.—Hexasaccharides **F** and **J** are similar to **D** except for the lack of a sulfate group at the C-6 position of the GlcNAc residue in **F** and a sulfate group at the C-2 position of the iduronic acid in **J**. The absence of a sulfate group at the C-6 position of the GlcNAc residue is indicated by the chemical shift of H-6 being upfield ~0.4 ppm in comparison with that of **D**. The H-2 resonance at 3.768 ppm indicates the lack of a 2-*O*-sulfate group on the iduronic acid next to the GlcNAc. The structure of **F** was determined to be: ΔUA(2S) – GlcNS(6S) – IdoA(2S) – GlcNAc – GlcA–GlcNS(6S); that of **J** was determined to be ΔUA(2S)–GlcNS(6S)–IdoA–GlcNAc(6S)–GlcA–GlcNS(6S).

Hexasaccharides **G** *and* **I**.—The presence of a GlcNAc residue at the reducing end of both hexasaccharides is indicated by the ~0.4–0.6 ppm downfield shift of the resonances for the H-2 protons of both residues, depending on whether they are in the α or β conformation. The observation of the additional β anomer is further evidence of *N*-acetylation.[43] Although the chemical shift of the H-6 protons cannot be determined due to resonance overlap, the absence of a resonance at 4.2–4.4 ppm for these terminal residues indicates the lack of a sulfate group at the 6-position. Likewise, a 0.2 ppm upfield shift of the H-1 resonance indicates the lack of a sulfate group at the 2-position of the uronic acid residue next to the reducing end. The structure of **G** was determined to be ΔUA(2S)–GlcNS(6S)–IdoA(2S)–GlcNS(6S)–IdoA–GlcNAc; that of **I** was determined to be ΔUA(2S)–GlcNS(6S)–IdoA(2S)–GlcNS–IdoA–GlcNAc.

Oligosaccharide **L**.—There are two distinct parts to **L**. Proton chemical shift data for the first part are similar to that for **K**, except for the absence of the sulfate group on C-6 of Glc-d. In addition, 1D and 2D TOCSY spectra clearly show the presence of four additional spin systems in the 4.7–4.2 ppm region; the 1D spectrum is shown in Fig. 9. These resonances are for the trisaccharide linker sequence and for serine of the protein. The linker residues were identified as Gal, Gal, and Xyl on the basis of chemical shift data obtained from the TOCSY traces through the anomeric proton resonances and comparison with literature data.[36,49] Serine was also identified from TOCSY traces. ROESY crosspeaks between GlcA-H-1 and Gal-1-H-3, Gal-1-H-

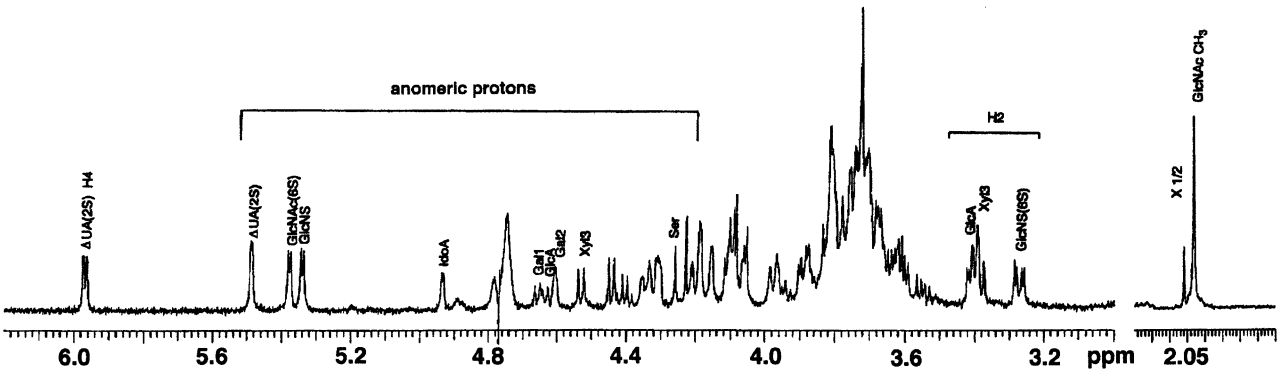

Fig. 9. 500 MHz ^{1}H NMR spectrum of oligosaccharide **L**. Resonances of the anomeric protons and H-2 protons of selected monosaccharides, including those of the Gal-Gal-Xyl linker sequence, are identified.

1 and Gal-2-H-3, Gal-2-H-1 and Xyl-3-H-4 indicate the sequence of **L** to be: ΔUA(2S)–GlcNS(6S)–IdoA–GlcNAc–GlcA–Gal–Gal–Xyl–Ser.

4. Discussion

The primary structure of heparin consists of the repeating disaccharide region and the protein linkage region. The repeating disaccharide region can be subdivided into highly sulfated regular regions or domains, which are comprised primarily of the repeating (1→4)-linked disaccharide IdoA(2S)–GlcNS(6S), and the irregular regions. Several disaccharide sequences which differ in extent of 2-*O*-sulfation of the hexuronic acids, 6-*O*- and 3-*O*-sulfation of glucosamine, and *N*-sulfation versus *N*-acetylation of glucosamine are possible in both the regular and irregular regions. Several of the many possible oligosaccharide sequences have been identified through the isolation and characterization of heparin-derived tetra-, hexa-, and octasaccharides.[20,22–25,29–31,42–49]

Of the heparin-derived oligosaccharides isolated and characterized in this study, **E**, **G**, **H**, and **I** were isolated and characterized for the first time as discrete structures. These four hexasaccharides, together with **A** and **C**, share the common tetrasulfated hexasaccharide core sequence ΔUA(2S)–GlcNS–IdoA(2S)–GlcNS–IdoA–GlcN. They differ from each other in the degree of *O*-sulfation on GlcN-b, GlcN-d, and IdoA-e, and *N*-sulfation versus *N*-acetylation of GlcN-f. **A**, **C**, **E**– and **H** are from the regular region. **A** is comprised of three repeats of the fully sulfated disaccharide IdoA(2S)–GlcNS(6S), while **C**, **E**, and **H** are under-sulfated at the 6-O position of one, two and three GlcNS residues, respectively. Structures **E** and **H**, with two and three adjacent IdoA(2S)–GlcNS disaccharides, respectively, are unusual since the IdoA(2S)–GlcNS disaccharide can act as a substrate for 6-*O*-sulfotransferase.[50] **G** and **I** are unusual, in comparison to hexasaccharides reported previously, in that they have a GlcNAc residue at the reducing end.[24] Based on the specificity of heparinase I mentioned above, it is likely that **G** and **I**, with GlcNAc at the reducing terminus, were produced by a heparinase III impurity in the heparinase I preparation.[29]

B, **D**, **F**, and **J** share the common core sequence ΔUA(2S)–GlcNS(6S)–IdoA–GlcN–GlcA–GlcNS(6S), with additional sulfate groups on IdoA-c, and 6-*O*-sulfate and *N*-acetyl or *N*-sulfate groups on GlcN-d. With the internal GlcNAc–GlcA disaccharide sequence, **D**, **F**, and **J** are considered to be from the irregular region.[42] No oligosaccharides with the reverse sequence, –GlcA–GlcNAc–, were identified, consistent with the conclusion that the –GlcNAc–GlcA– sequence does not serve as a substrate for the epimerase involved in heparin–heparan sulfate biosynthesis.[42,51]

L is from the protein linkage region. Pentasaccharide **K** is presumably derived from the cleavage site of endogenous *endo*-β-glucuronidase.[42]

The twelve oligosaccharides isolated and characterized in this study were prepared by digestion of porcine intestinal mucosal heparin with heparinase I in the presence of histamine, which binds site specifically to heparin.[31,32] The ^{1}H NMR spectra in Fig. 3 show that histamine alters the product profile of heparinase I-catalyzed depolymerization of heparin, the result of which is formation of the new hexasaccharides **E**, **G**, **H**, and **I** in sufficient quantities for isolation and characterization. Histamine presumably alters the product profile distribution by blocking potential cleavage sites. For example, the GlcNS-(1→4)-IdoA glycosidic bonds in **E**, **G**, **H**, and **I** are normally readily cleaved by heparinase I.[42,52] The diprotonated form of histamine binds site-specifically to the ΔUA(2S)–GlcNS(6S)–IdoA and IdoA–GlcNS–IdoA trisaccharide sequences within heparin, but not to the IdoA–GlcNS–GlcA trisaccharide sequence. Thus, histamine will bind to the ΔUA(2S)–GlcNS(6S)–IdoA trisaccharide sequences of **B**, **D**, **F**, and **J**, with the imidazolium ring located at the

GlcNS(6S) residue. The other six hexasaccharides each have two histamine binding sites formed by the ΔUA(2S)–GlcNS–IdoA(2S) and IdoA(2S)–GlcNS–IdoA trisaccharide sequences.

The time course data in Fig. 5 and the GPC data in Fig. 1 indicate that histamine increases the rate and extent of heparinase I-catalyzed depolymerization of heparin. Because the site-specific binding of histamine presumably blocks potential cleavage sites, the increased rate and extent of reaction were unexpected. We propose that the origin of the increased rate and extent of depolymerizatyion can be found in the properties of histidine-203, which together with cysteine-135 forms the catalytic site of heparinase I.[53,54] We have shown previously that the imidazolium side chain of histidine in peptides can bind site-specifically to heparin, in the same manner as the imidazolium group of histamine.[55] If oligosaccharides produced by heparinase I-catalyzed cleavage bind nonproductively to the imidazolium side chain of His-203, this would have the effect of inhibiting the activity of heparinase I. However, competitive binding of these oligosaccharides by the added histamine would reduce the extent of inhibition, with the result that the rate of depolymerization is increased.

Acknowledgements

This work was supported in part by the National Institutes of Health Grant HL56588 and by the University of California, Riverside, Committee on Research. Funding for the Varian Unity Inova 500 spectrometer was provided in part by NSF-ARI Grant 9601831.

References

1. Bourin M.-C.; Lindahl U. *Biochem. J.* **1993**, *289*, 313–330.
2. Olivercrona T.; Bengtsson-Olivercrona G. Heparin and Lipases. In *Heparin*: *Chemical and Biological Properties, Clinical Applications*; Lane D.; Lindahl U., Eds.; CRC Press: Boca Raton, FL, 1989; pp. 335–361.
3. Gallagher J. T.; Lyon M.; Steward W. P. *Biochem. J.* **1986**, *236*, 313–325.
4. Kazatchkine M. D.; Fearon D. T.; Metcalfe D. D.; Rosenberg R. D.; Austen F. K. *J. Clin. Invest.* **1981**, *67*, 223–228.
5. Sharath M. D.; Merchant Z. M.; Kim Y. S.; Rice K. G.; Linhardt R. J.; Weiler J. M. *Immunopharmacology* **1985**, *9*, 73–80.
6. Castellot J. J.; Wright T. C.; Karnovsky J. *Semin. Thromb. Hemost.* **1987**, *13*, 489–503.
7. Wright T. C.; Castello J. J.; Petitou M.; Lormeau J.-C.; Choay J.; Karnovsky M. J. *J. Biol. Chem.* **1989**, *264*, 1534–1542.
8. Folkman J.; Langer R.; Linhardt R. J.; Handeschild C.; Taylor S. *Science* **1983**, *221*, 719–725.
9. Crum R.; Szabo S.; Folkman J. *Science* **1985**, *230*, 1375–1378.
10. Holondniy M.; Kim S.; Katzenstein D.; Konrad M.; Groves E. T.; Merigan T. C. *J. Clin. Microbiol.* **1991**, *29*, 676–679.
11. Shieh M.-T.; Spear P. G. J. *Virology* **1994**, *68*, 1224–1228.
12. Capila I.; Linhardt R. J. *Angew. Chem., Int. Ed. Engl.* **2002**, *41*, 390–412.
13. Linhardt R. J.; Toida T. Heparin Oligosaccharides: New Analogues Development and Applications. In *Carbohydrates in Drug Design*; Witczak Z. B.; Nieforth K. A., Eds.; Marcel Dekker: New York, 1997; pp. 277–341.
14. Björk I.; Olson S. T.; Shore J. D. Molecular Mechanisms of the Accelerating Effect of Heparin on the Reactions Between Antithrombin and Clotting Proteinases. In *Heparin*: *Chemical and Biological Properties, Clinical Applications*; Lane D. A.; Lindahl U., Eds.; CRC Press: Boca Raton, FL, 1989; pp. 229–255.
15. Lam L. H.; Silbert J. E.; Rosenberg R. D. *Biochem. Biophys. Res. Commun.* **1976**, *69*, 570–577.
16. Höök M.; Björk I.; Hopwood J.; Lindahl U. *FEBS Lett.* **1976**, *66*, 90–93.
17. Rosenberg R. D.; Lam L. *Proc. Natl. Acad. Sci. USA* **1979**, *76*, 1218–1222.
18. Lindahl U.; Backstrom G.; Höök M.; Thunberg L.; Fransson L.-A.; Linker A. *Proc. Natl. Acad. Sci. USA* **1979**, *76*, 3198–3202.
19. Lindahl U.; Thunberg L.; Bäckström G.; Riesenfeld J.; Nordling K.; Björk I. *J. Biol. Chem.* **1984**, *259*, 12368–12376.
20. Linhardt R. J.; Loganathan D. Heparin, Heparinoids and Heparin Oligosaccharides: Structure and Biological Activities. In *Biomimetic Polymers*; Gebelein C. G., Ed.; Plenum Press: New York, 1990; pp. 135–173.
21. Spillman D.; Lindahl U. *Curr. Opin. Struct. Biol.* **1994**, *4*, 677–682.
22. Gettins P.; Horne A. *Carbohydr. Res.* **1992**, *223*, 81–98.
23. Pervin A.; Gallo C.; Jandik K. A.; Han X. J.; Linhardt R. J. *Glycobiology* **1995**, *5*, 83–95.
24. Larnkjaer A.; Hansen S. H.; Østergaard P. B. *Carbohydr. Res.* **1995**, *266*, 37–52.
25. Yamada S.; Murakami T.; Tsuda H.; Yoshida K.; Sugahara K. *J. Biol. Chem.* **1995**, *270*, 8696–8705.
26. Casu B. Methods of Structural Analysis. In *Heparin*: *Chemical and Biological Properties, Clinical Applications*; Lane D. A.; Lindahl U., Eds.; CRC Press: Boca Raton, FL, 1989; pp. 25–49.
27. Gatti G.; Casu B.; Hamer G. K.; Perlin A. S. *Macromolecules* **1979**, *12*, 1001–1007.
28. Rice K.; Linhardt R. *Carbohydr. Res.* **1989**, *190*, 219–233.
29. Desai U. R.; Wang H.-M.; Linhardt R. J. *Biochemistry* **1993**, *32*, 8140–8145.
30. Linhardt R. J. Chemical and Enzymatic Methods for the Depolymerization and Modification of Heparin. In *Carbohydrates—Synthetic Methods and Applications in Medicinal Chemistry*; Weinheim H.; Ogura A.; Hasegawa T. S.; Suami T., Eds.; Kodansha/VCH: Tokyo, 1992; pp. 385–401.
31. Rabenstein D. L.; Bratt P.; Schierling T. D.; Robert J. M.; Guo W. *J. Am. Chem. Soc.* **1992**, *114*, 3278–3285.
32. Chuang W.-L.; Christ M. D.; Peng J.; Rabenstein D. L. *Biochemistry* **2000**, *39*, 3542–3555.
33. Chuang W.-L.; McAllister H.; Rabenstein D. L. *J. Chromatogr. A* **2001**, *932*, 65–74.

34. Venkataraman G.; Shriver Z.; Raman G.; Sasisekharan R. *Science* **1999**, *286*, 537–542.
35. Horne A.; Gettins P. *Carbohydr. Res.* **1991**, *225*, 43–57.
36. Sugahara K.; Tsuda H.; Yoshid K.; Yamada S.; Beer T. De.; Vliegenthart F. G. *J. Biol. Chem.* **1995**, *270*, 22914–22923.
37. Bax A.; Davis D. G. *J. Magn. Reson.* **1985**, *65*, 355–360.
38. Davis D. G.; Bax A. *J. Am. Chem. Soc.* **1985**, *107*, 2820–2821.
39. Bothner-By A. A.; Stephens R. L.; Lee J.-M.; Warren C. D.; Jeanloz R. W. *J. Am. Chem. Soc.* **1984**, *106*, 811–813.
40. Bax A.; Davis D. G. *J. Magn. Reson.* **1985**, *63*, 207–213.
41. Chuang W.-L.; Christ M. D.; Rabenstein D. L. *Anal. Chem.* **2001**, *73*, 2310–2316.
42. Yamada S.; Yamane Y.; Tsuda H.; Yoshida K.; Sugahara K. *J. Biol. Chem.* **1998**, *273*, 1863–1871.
43. Hileman R. E.; Smith A. E.; Toida T.; Linhardt R. J. *Glycobiology* **1997**, *7*, 231–239.
44. Tsuda H.; Yamada S.; Yamane Y.; Yoshida K.; Hopwood J. J.; Sugahara K. *J. Biol. Chem.* **1996**, *271*, 10495–10502.
45. Yamada S.; Sakamoto K.; Tsuda H.; Yoshida K.; Sugiura M.; Sugahara K. *Biochemistry* **1999**, *38*, 838–847.
46. Chai W.; Hounsell E. F.; Bauer C. J.; Lawson A. M. *Carbohydr. Res.* **1995**, *269*, 139–156.
47. Toida T.; Hileman R. E.; Smith A. E.; Vlahova P. I.; Linhardt R. J. *J. Biol. Chem.* **1996**, *271*, 32040–32047.
48. Linhardt R. J.; Rice K. G.; Merchant Z. M.; Kim Y. S.; Lohse D. L. *J. Biol. Chem.* **1986**, *261*, 14448–14454.
49. Sugahara K.; Yamada S.; Yoshida K.; de Waard P.; Vliegenhart J. F. G. *J. Biol. Chem.* **1992**, *267*, 1528–1533.
50. Conrad H. E. *Heparin-Binding Proteins*; Academic Press: San Diego, CA, 1998; p. 33.
51. Jacobson I.; Lindahl U.; Jensen J. W.; Rodén L.; Prihar H.; Feingold D. S. *J. Biol. Chem.* **1984**, *259*, 1056–1063.
52. Desai U. R.; Wang H. M.; Linhardt R. J. *Arch. Biochem. Biophys.* **1993**, *306*, 461–468.
53. Godvarti R.; Cooney C. L.; Langer R.; Sasisekharan R. *Biochemistry* **1996**, *35*, 6846–6852.
54. Sasisekharan R.; Venkataraman G.; Godvarti R.; Ernst S.; Cooney C. L.; Langer R. *J. Biol. Chem.* **1996**, *271*, 3124–3131.
55. Rabenstein D. L.; Robert J. M.; Hari S. *FEBS Lett.* **1995**, *376*, 216–220.